International Journal for Multidisciplinary Research (IJFMR)
E-ISSN: 2582-2160 ● Website: www.ijfmr.com ● Email: editor@ijfmr.com

Study On the Synthesis and Characterization of Zeolites

Mr.Kamlesh Sahu

Research Scholar Jiwaji University
Gwalior, M.P.

ABSTRACT

Zeolites, which are crystalline aluminosilicates with porosity structures that are clearly characterized, are components that are necessary for catalytic processes. The purpose of this study is to discuss research that has been conducted on the synthesis, characterization, and applications of zeolites in catalysis. There are several different synthesis strategies that are utilized in order to produce zeolites that possess the chemical and structural properties that are required. These processes include hydrothermal and ion-exchange methods. Through characterisation using cutting-edge techniques such as Fourier-transform infrared spectroscopy (FTIR), scanning electron microscopy (SEM), and X-ray diffraction (XRD), it is possible to gain a deeper comprehension of the surface characteristics, porosity, and crystal structures of the zeolites. A number of significant reactions, including hydrocracking, isomerization, and catalytic cracking, are implemented in order to evaluate the catalytic efficiency of the zeolites that are created. Both the properties of the zeolite and the factors that contribute to its production are investigated in relation to the catalytic activity, selectivity, and stability. Based on the findings, it is clear that the catalytic efficiency and effectiveness of zeolites may be significantly adjusted by modifying their composition and the manufacturing process. The results of this study demonstrate that in order to find the most effective zeolite catalysts, rigorous characterization and specialized manufacture are required. The findings give significant information that may be utilized for the purpose of enhancing catalytic processes in industrial settings and indicate to prospective possibilities for additional research in zeolite-based catalysis systems.

Keywords: Zeolites, Synthesis, Characterization, Catalytic property, crystalline alumino- silicates

1. INTRODUCTION

Zeolites, three-dimensional, porous hydrated aluminosilicates, can contain alkaline earth element cations (calcium, magnesium, barium, strontium, and sodium) and other monovalent or multivalent metals. Zeolites can shed and absorb water in amounts more than 30% of their dry weight due to their diverse structure, which has massive open spaces and channels. In zeolites, the principal building units (PBU) are tetrahedra of silicon [SiO4] and aluminum [AlO4] joined by oxygen atoms that are shared by the PBU and the subsidiary building units. Löwenstein's rule states that Si-O-Si tetrahedra can be put adjacent to each other, while Al-O tetrahedra can only be linked to Si-O-Al. When Al3+ is placed in the Si4+ cation's tetrahedral position, surplus electrons induce a negative charge. Na+, K+, NH4+, H+, Ca2+, Sr2+, and

Mg2+ are exchangeable cations that counteract this. These off-grid cations and water molecules can move freely within the mineral and exchange with other ions in the environment due to the aluminosilicate skeleton. Due to the unequal distribution of tetrahedra, zeolites have a network of structural gaps and channels of variable widths that contain zeolitic water at room temperature. Thermal treatment quickly removes water without altering zeolite's crystal structure (Figure 1). Released pores can absorb water or other adsorbates [1,2].

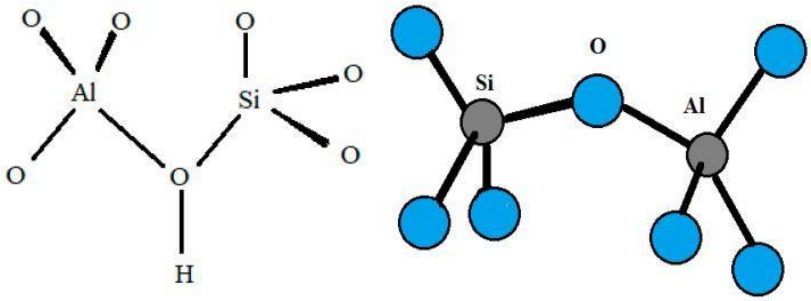

Figure 1 Scheme of silicon and aluminum tetrahedra in the zeolite structure.

An example of an elementary cell and channel system of FAU, LTA, and MFI zeolites is shown in Figure 2.

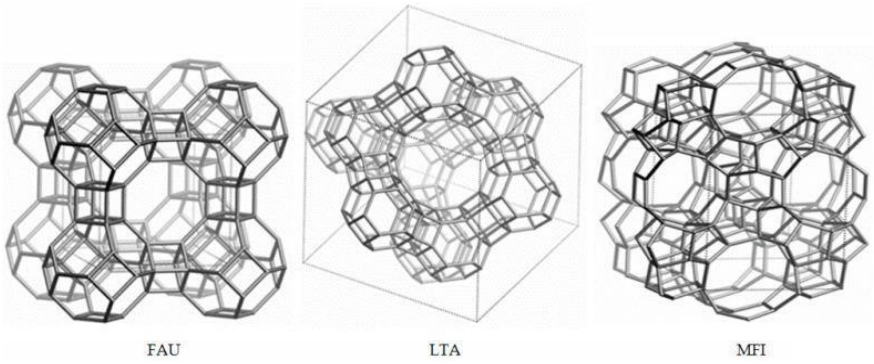

Figure 2 Elemental cell and channel system of FAU, LTA, and MFI zeolites.

Swedish mineralogist Axel Frederic von Cronstedt discovered stilbite, the first zeolite, in 1756 [3]. Zeolites are formed from volcanic rocks and ash and acidic, salty water. Science knows about 50 natural zeolites, including clinoptilolite, analcime, mordenite, and chabazite, and 150 synthetic ones. People use natural and synthetic zeolites in different ways. Manufactured zeolites are used more because natural ones may contain other minerals or metals [3]. Synthetic zeolites often outperform natural ones in physical and chemical properties. Synthetic zeolites are better at adsorbing heavier compounds like diesel oil than natural ones due to their larger pore size and reaction environment stability. Synthetic materials remove heavy metal ions and radioactive contaminants faster than natural zeolites.

Properties and Classification of Zeolites

Due to its skeleton channels and chambers, zeolite has several beneficial physicochemical properties. Zeolite surfaces have active acid-base or oxidation-reduction centers. These explain their remarkable catalytic and adsorption activities [4]. Zeolites exhibit micropores with

volumes of 0.10 to 0.35 cm3 g−1 and diameters of 0.3 to 1.0 nm [3]. Table 1 lists the various zeolites by pore size.

Table 1 Classification of zeolites based on the size of pores in the structure.

Type of Zeolite	Membered Rings (MR)	Pore Diameter [nm]	Example of Zeolite
With small pore size	8	0.3–0.45	zeolite A
With medium pore size	10	0.45–0.6	ZSM-5, MCM 22
With large pore size	12	0.6–0.8	zeolite X, Y
With very large pore size and zeolite-like materials	14	0.8–1.0	UTD 1 (14 MR) VIP 5 (18 MR) Cloverite (20 MR)

Zeolites are further classified by Si/Al molar ratio. According to Szostak [5], this ratio determines zeolites' physicochemical properties (Figure 3). The Si/Al ratio classifies zeolites by silicon concentration (Table 2).

Increased Si/Al ratio renders zeolite structure thermally stable, reducing amorphization and dealumination. According to this correlation, low-silicon zeolites can lose structure at 700 °C, whereas high-silicon ones can withstand 1300 °C. Hydrophilicity and ion exchange capacity are further features of low-silicon zeolites. Due to their greater hydrophobicity and active center power, high-silicon zeolites are ideal for catalysis. Acidity increases proportionally with Si/Al. However, under the same conditions, the structure's off-grid exchangeable cations decrease, lowering its ion exchange capacity. This capacity is linked to the quantity of AlO4− tetrahedra in the zeolite skeleton.

Zeolites have many benefits due to their unique structure. They are environmentally friendly ion exchangers, molecular sieves, catalysts, and water and uncharged molecule adsorbents. Significant properties of zeolite framework include a cation exchange capacity of 200-300 cmol(+) kg−1 and a large internal surface area of several hundred m2 g−1 [6]. Moreover, zeolites have low bulk density (0.8-1.5 Mg m−3) and crystal density (1.9-2.2 Mg m−3) [6]. Zeolites' unique physicochemical properties have made them helpful in many industries, including agriculture and environmental protection.

Table 2 Classification of zeolites in terms of Si/Al ratio values

Type of Zeolite	Si/Al Ratio	Example of Zeolite

Low silicon	1.0–1.5	4A, X, UZM-4, UZM-5
Medium silicon	~2.0–5.0	mordenite, zeolite Y, L
High silicon	>10	Beta, ZSM-5, ZSM-12
Silica molecular sieves	>100	silicites

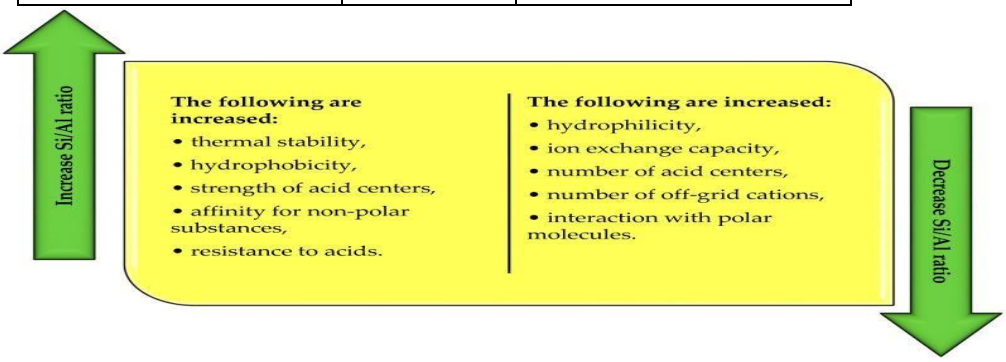

Figure 3 Changes in the physicochemical properties of zeolites as a function of the molar ratio of silicon to aluminum.

OBJECTIVES

1. To study the synthesis and characterization of zeolites
2. To study the application of zeolites as catalysts

ZEOLITE SYNTHESIS METHODS

Public interest in synthetic zeolites has grown due to their industrial applications. Recent advances in synthetic technologies allow for the synthesis of zeolite material with customizable features. The zeolite process begins with silica and clay minerals, which include silicon and aluminum. Red sludge, glass pellets, and fly ash all have comparable chemical compositions to zeolites and can be used as reactants.

Hydrothermal synthesis of zeolites in water is the most common method. Organic solvents including pyridine, hydrocarbons, ethylene glycol, and alcohols like methanol and ethanol are employed in solvothermal synthesis, which can involve water. The ionothermal technique uses ionic liquids because of their low melting point, less than 100 °C. In theory, all solvothermal procedures incorporate hydrothermal and ionothermal processes, but not in practice. The prior classification of zeolite synthesis methods shows this.

1. Hydrothermal Synthesis

Traditional zeolite synthesis includes a long hydrothermal process in a closed system at 90– 150 °C and 1–15 bar in an alkaline atmosphere. The process usually takes 24–96 hours.

Crystalline aluminosilicate is made from organic molecules, metal cations, and hydrogel in this multi-step process. Most aluminosilicate hydrogels are made from silicon (water glass, kaolinite, and SO2 colloid) and aluminum (aluminate, aluminum nitrate, and aluminum sulfate). Reactants are usually manufactured from natural clays like halloysite or kaolin or waste products like fly ash, rice husk, or paper sludge because pure substrates are expensive. Crystal nuclei form fastest in the early phases of crystallization. Zeolites are hydrothermally synthesized at temperatures of 100 °C to generate crystals ranging from 0.1 to 10 μm in size. Zeolite (Y, X, A, P), chabazite, phillipsite, faujasite, and Na-P1 can be hydrothermally produced. Johnson and Arshad [7] noted that hydrothermal synthesis of kaolin-based zeolites needs careful consideration of many important parameters:

(a) Si/Al molar ratio: low (≤ 5) yields SAPO, LTA, and zeolites X; high (≥ 5) yields beta, ZSM-5, and zeolite Y;

(b) NaOH concentration: optimum ≤ 3 Mol L−1 for relative crystallinity and impurity formation;

(c) Crystallization temperature: 70 °C.

Novembre et al. [8] hydrothermally generated Na-X zeolite from naturally zeolitized alkaline volcanic rock and siliceous silica. The experiment used a 3 Mol L−1 sodium hydroxide solution at 80 °C. The Na-X zeolite was synthesized after 5 hours and crystallized after 18 hours. Zeolite generated had 500-hour stability.

2. Various Techniques of Hydrothermal Synthesis

2.1. Alkali Fusion

Traditional hydrothermal treatment follows zeolite fusion. This procedure activates zeolitization by fusing raw material with an alkali such solid sodium hydroxide. The synthesis process begins with thermal activation, which requires heating the starting material to 500–650
°C. The reaction mixture is then aged for several to tens of hours at 20–50 degrees Celsius. Final crystallization occurs by heating the reaction mixture to 100 °C for 24–48 hours [9]. To boost zeolite production during chemical synthesis, sodium hydroxide is employed as the base during fusion to stabilize the subunit's crystal structure.

The above technique uses sodium silicate, colloidal silica, sodium aluminate, and aluminum isopropanolate [9]. Quality of the final synthesis product depends on many aspects, including the molar ratio of Na2O to SiO2, Al2O3, and water, activation temperature and duration, reaction mixture aging time, and crystallization temperature and duration. According to Aylele et al. [10], alkaline fusion in zeolite A synthesis can use low-quality primary kaolin without purification, unlike hydrothermal synthesis. Lee et al. [11] shown that hydrothermal and alkaline fusion may synthesize Na-A zeolite (Z-S1) from scoria, a volcanic rock. Their research shows that particle size decreases with alkali content in the medium and that managing the NaOH/precursor ratio is essential for high zeolite crystallinity.

2.2. Alkaline Activation

Zeolites can be synthesized by alkaline activation crystallization. This approach is commonly used to produce geopolymers, inorganic polymers formed at low temperatures (<100 °C) from mineral molecules bound by covalent bonds. Geopolymers are formed by alkaline solutions reacting with low-calcium aluminosilicates such silica fly ash. Alkaline activation uses a concentrated base—hydroxide, silicate, carbonate, or sulfate [30]. Amorphous or subcrystalline aluminosilicate structures with polymeric Si-O-Al-O connections emerge when reactive aluminosilicates dissolve in aqueous alkaline solutions and [SiO4]4− and [AlO4]5− tetrahedra link corners by polycondensation. Garcia-Lodeiro et al. [12] explained fly ash's aluminosilicate phase alkaline activation. These authors believe alkaline activation creates amorphous hydrated aluminosilicates, zeolites, and gels in high-aluminosilicate materials. Zeolites formed via reaction include hydrosodalite, zeolite P, chabazite-Na, and faujasite-Ca. The simultaneous occurrence of geopolymerization reaction stages confuses its already- mysterious mechanism. However, the three main phases are:

(1) A strong alkaline solution dissolves silica and alumina, breaking down solid aluminosilicates into silicates, aluminosilicates, and aluminates.

(2) Solution diffusion of solutes causes polycondensation and gel formation. Geopolymer inorganic gel.

(3) Gel hardens, polymerizing. By connecting, crosslinking, and rearranging the geopolymer gel network, this technique creates a three-dimensional aluminosilicate structure.

Alkaline activation of natural zeolite created geopolymers, according to Villa et al. [13]. They used sodium silicate and sodium hydroxide in 0.4, 1.5, 5, 10, and 15 amounts as activators in a 7 M sodium hydroxide solution. The activator/precursor ratio was 0.6, although setup and curing temperatures and periods were adjustable. Testing showed that activator/precursor ratio and curing period increased material mechanical strength. The ideal circumstances were 90 days and 40 °C.

Alkaline activators' monovalent cations (Na+ or K+) from KOH or Na2SiO3 compensate for the negative charge, enabling new structure formation. Alkaline activation is a polycondensation reaction. Adding alkali metal hydroxide and silicate boosts the process. Alkali metal cations are critical to synthesis curing and crystal formation. Alkali-activated materials have low heat conductivity, quick curing, durability, fire and corrosion resistance, and high mechanical strength. These advantages make the above materials popular in thermal insulation, construction, catalysts, and membranes.

3. Molten Salt Method

Park et al. [14] invented this zeolite synthesis method. Anhydrous conditions and temperatures over 250 °C are needed to react fly ash with NaOH-NaNO3 or NaOH-KNO3. Benefits of this technology include low temperatures, simple and adaptable application, and good cost/purity

ratio of products achieved in one process. Anhydrous conditions prevent alkaline liquid waste, the synthesis time is faster than other methods, and this method can synthesize zeolites from several mineral wastes. Without enough water, reactants may not make enough contact during crystallization. This slows precursor-to-product conversion and produces uneven zeolite morphology. Park et al. [14] tested zeolite fly ash with different salt solutions. Mineralizers were NaOH, KOH, or NH4F, and stabilizers were NaNO3, KNO3, or NH4NO3. The 350 °C reaction mixture contained 0.7 g fly ash, 0.3 g alkali, and 1 g salt. Sodalite and cancrinite were the authors' key zeolite phases.

4. Microwave Assisted Synthesis

Zeolites can also be synthesized by microwave irradiation. This simple method can speed up zeolite synthesis, uniformize size and content, and make precursor gel dissolve faster. According to Panzarella et al. [15], microwave-assisted synthesis efficacy depends on reaction vessel size and reaction mixture volume. Microwave-heated materials include zeolite A, ZSM- 5, faujazyite, analcime, AIPO4-5, and VPI-5. Microwave radiation in zeolite synthesis has various advantages:

(a) homogeneous heating throughout the reaction mixture,

(b) high reaction efficiency,

(c) controllability of morphology, phase purity, and pore size,

(d) lightning-fast production of crystallization nuclei, and

(e) significantly faster heating of the reaction mixture than conventional methods.

Anuwattana et al. found that microwave heating at 150 °C (2.45 GHz, 1200 W) tripled ZSM-5 zeolite synthesis from iron slag compared to hydrothermal heating [16]. Furthermore, it led to the fabrication of smaller ZSM-5 particles (0.3 μm vs. 3 μm).

5. Other Methods

An innovative method for synthesising zeolites is using an inert mesoporous substance, commonly carbon. Zeolite is crystallized in an inert matrix's porous network as a precursor. This stops crystals from growing beyond pores. After that, 550 °C pyrolysis removes crystals from the matrix. No doubt, confined space synthesis provides these benefits:

(a) high reproducibility,

(b) control of the maximum crystal size by the size of the matrix mesopores,

(c) high purity of the obtained samples,

(d) the possibility of selecting the synthesis conditions to obtain highly crystalline zeolites.

This method produces zeolites with the same number of acid sites and high specific surface area as large zeolite crystals.

Vapour phase transport synthesis uses dry aluminosilicate gels, amines, and water to make zeolites. According to Kim et al. [17], water vapor condenses on the precursor's micropores to establish a liquid-vapor equilibrium. Organic cations then react with gel silica. Crystals arise from crystal nuclei on the precursor. Water content in the solvent mixture during VPT manufacturing is the main factor affecting crystallization. Water consumption determines product crystallinity and structural complexity. In addition to affecting crystallization and particle size, alkalinity is important.

Growing trend: mechanochemical synthesis of zeolites. The crude precursors are exposed to mechanical energy alone in a solvent-free or low-solvent environment. This method controls amorphization to reduce energy, administrative costs, and waste while affecting active site type, density, and availability.

CHARACTERIZATION OF ZEOLITE

1. Powder X-Ray Diffraction (XRD)

XRD can readily identify polluted states' crystalline structure. XRD can reveal zeolite crystal structure, size, defects, and heteroatom substitution. Melaningtyas et al. [18] used Bayat natural zeolite as a starting material and showed how pH affects the production of NaY zeolite with XRD patterns at pH 11–13. The XRD pattern of produced NaY was compared to IZA database NaP zeolite, confirming the findings (Figure 4). The graph revealed unformed NaY zeolite at pH 11 and 12. However, at 2θ values of 6.73°, 10.91°, 23.23°, and 27.47°, it resembled the typical NaY zeolite [18]. Non-Na cations such K+, Mg2+, Ca2+, and Fe2+ were left behind in pretreatment and are now present. NaY zeolite produced at pH 11 and 12 had an irregular baseline pattern, indicating a mixed amorphous component. Figure 4 demonstrates that zeolite NaY synthesised at pH 13 has a high crystalline structure like NaP. From the XRD patterns, the scientists concluded that the Bayat natural zeolite structure was transformed into zeolite NaY. The crystalline structure and pore homogeneity of zeolite NaY support the pH-sensitive pore size.

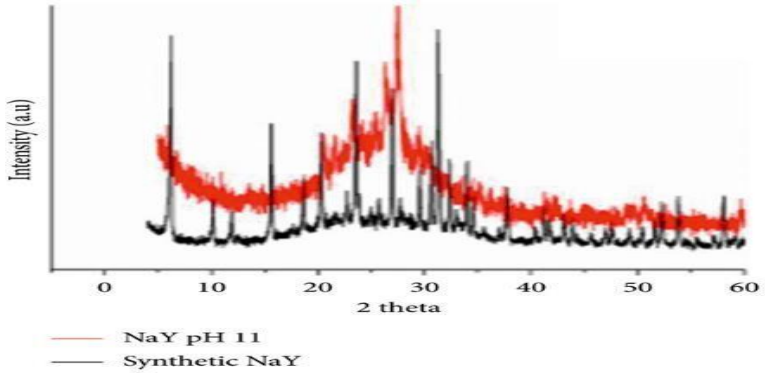

Figure 4 (a) Comparison of NaY zeolite XRD pattern at (a) pH 11, (b) pH 12, (c) pH 13, and (d) pH 13 with that of standard NaP zeolite.

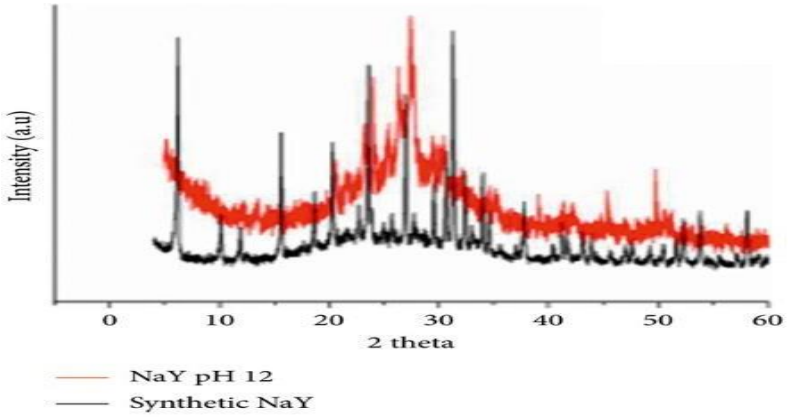

Figure 4 (b) Comparison of NaY zeolite XRD pattern at (a) pH 11, (b) pH 12, (c) pH 13, and (d) pH 13 with that of standard NaP zeolite.

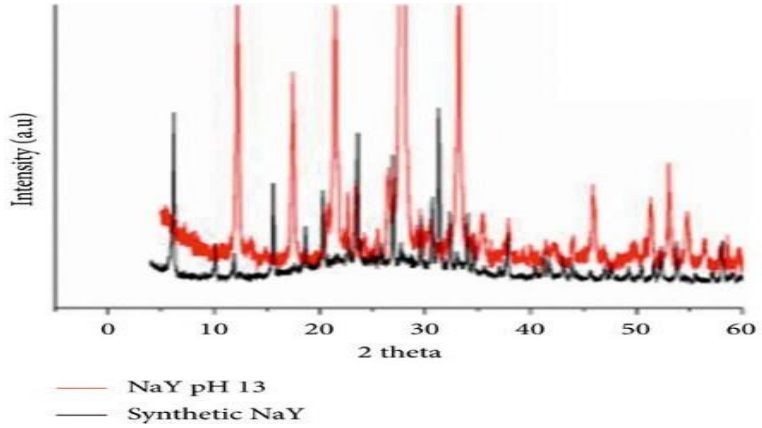

Figure 4 (c) Comparison of NaY zeolite XRD pattern at (a) pH 11, (b) pH 12, (c) pH 13, and (d) pH 13 with that of standard NaP zeolite.

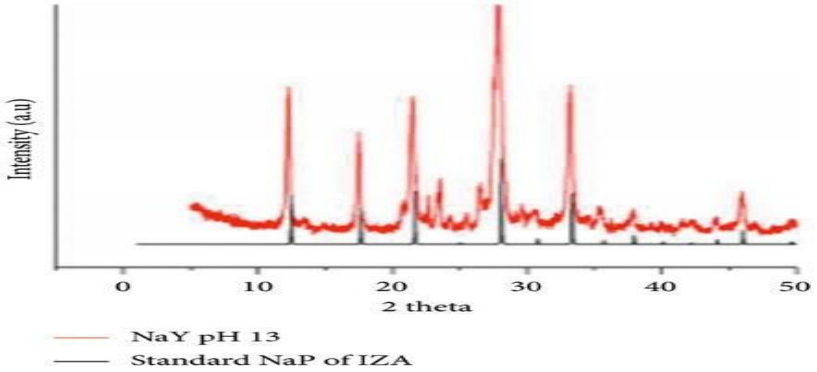

Figure 4 (d) Comparison of NaY zeolite XRD pattern at (a) pH 11, (b) pH 12, (c) pH 13, and (d) pH 13 with that of standard NaP zeolite.

2. Scanning Electron Microscopy (SEM)

SEM images can reveal a material's architecture and morphology. Chunfeng et al. [19] used scanning electron microscopy to compare zeolite A and X morphology. Zeolite A is chamfered- edged cubes, while

X is octahedral (Figure 5).

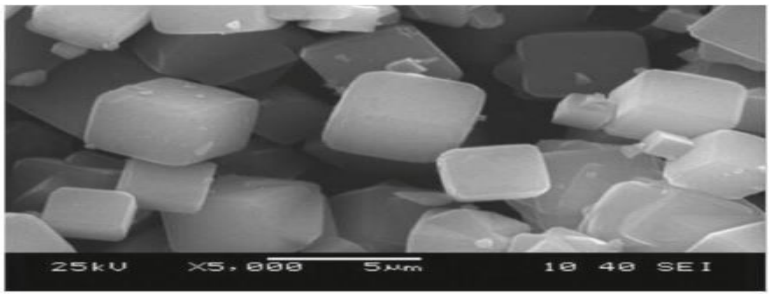

Figure 5 (a) SEM images of synthetic (a) zeolite A and (b) zeolite X.

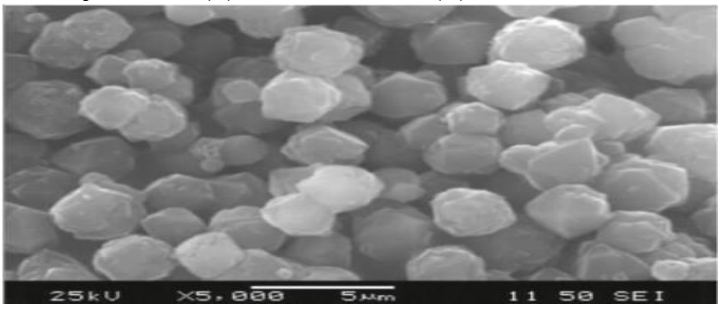

Figure 5 (b) SEM images of synthetic (a) zeolite A and (b) zeolite X

Magdalena [20] investigated zeolite growth rate by comparing one-step and multistep synthesis processes using SEM. Scientists found that multistep zeolite films had a clearer shape than one- step films. They also discovered that multistep synthesized films are better than one-step ones (Figure 6). The writers neglected particle agglomeration and diffusion limitation in their descriptions.

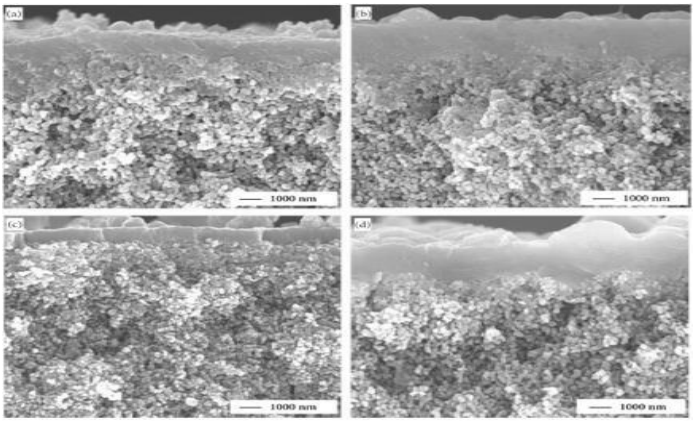

Figure 6 Side-view SEM images of membranes synthesized for 6 and 9 hours in one step (a and c) and 2 and 3 steps (b and d) at 75°C.

Omisanya et al. [21] compared kaolin sample zeolite A to commercially available 4A morphology. A plate-like structure for kaolinite clay shows silica and alumina are sliding, and the authors found cubic crystal structure in generated zeolite A and gel. SEM pictures of produced zeolite A showed regular-shaped particles of constant size. Both natural and chemically generated zeolites have an average crystal size of less than 20 µm, as revealed in scanning electron micrographs. Silica and alumina particles sliding over each other precluded the authors from utilizing the computational method to clarify the zeolite structure.

Nyankson et al. [22] used scanning electron microscopy to examine the form and texture of zeolites A, magnetite nanocomposite, and zeolite/Fe3O4 (Figure 7). SEN examination shows that zeolite crystals are cubic (Figure 7(a)), and the spherical Fe3O4 nanoparticles suggest magnetite was produced (Figure 7(b)). Magnetite nanoparticles incorporated into the zeolite framework altered the cubical geometry, as shown in Figure 7(c). This shows that zeolite and Fe3O4 nanoparticles bonded, changing the material's morphology and structure. Zeolite/Fe3O4 nanocomposites can distort owing to elongation, but the authors did not address this.

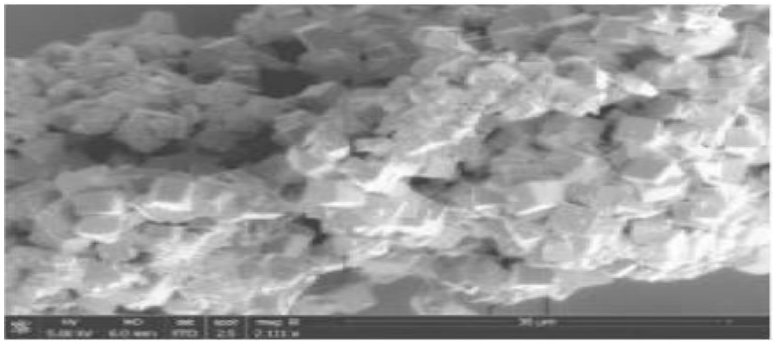

Figure 7 (a) SEM of (a) pure zeolite, (b) Fe_3O_4 NP, and (c) zeolite/magnetite nanocomposite (Z-Fe_3O_4 NP).

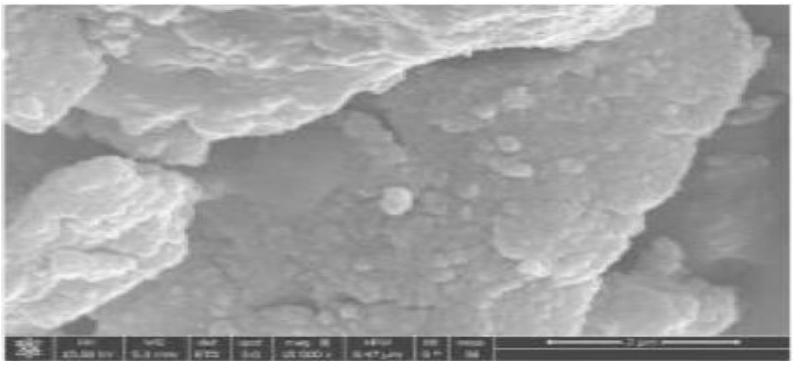

Figure 7 (b) SEM of (a) pure zeolite, (b) Fe_3O_4 NP, and (c) zeolite/magnetite nanocomposite (Z-Fe_3O_4 NP).

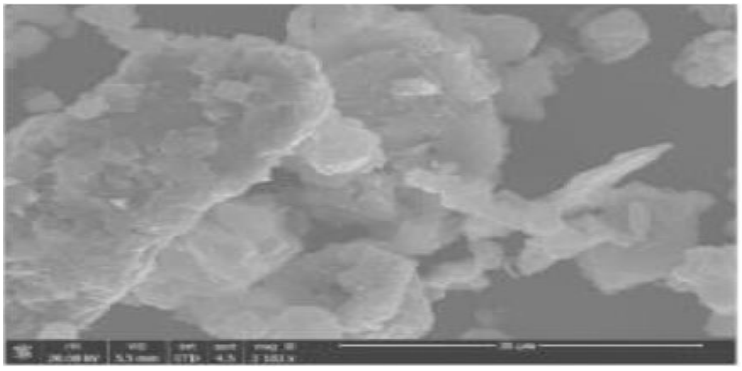

Figure 7 (c) SEM of (a) pure zeolite, (b) Fe_3O_4 NP, and (c) zeolite/magnetite nanocomposite (Z-Fe_3O_4 NP).

3. Fourier Transform Infrared (FTIR) Spectroscopy

Fourier transform infrared spectroscopy confirms silica-alumina basic vibrations in zeolite. The chemical process inside the zeolite framework can be anticipated and its functional units identified using Fourier transform infrared spectroscopy. FTIR can also show zeolite secondary building units [22].

Figure 7 shows Wang et al.'s FT-IR characterization and comparison of TiO2 and 10% Cr/TiO2 composite zeolites [23]. O-H bond stretching and bending are evidenced by high peaks at 3437 cm−1 and 1637 cm−1, respectively. Si-O-Si stretching is shown by the peak at 1049 cm−1, while bending vibrations of Si-O-Si and Ti-O are indicated by weak peaks between 800 and 400 cm−1. Thus, FT-IR peaks confirm the elemental connections of zeolite, TiO2/zeolite, and 10%Cr/TiO2/zeolite (Figure 8).

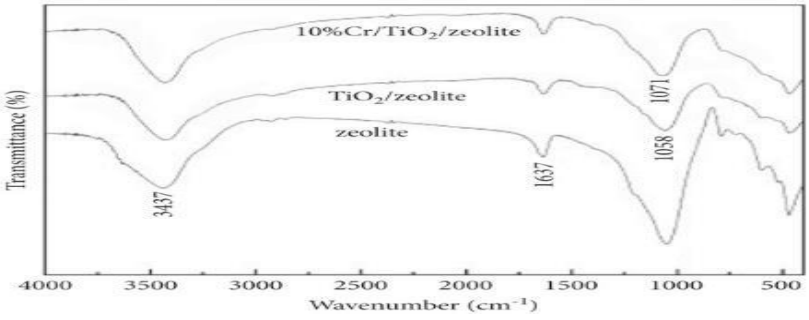

Figure 8 FT-IR spectra of zeolite, TiO_2/zeolite, and 10%Cr/TiO_2/zeolite.

FT-IR was used to compare Melaningtyas et al. [18] NaY zeolite to commercial NaY (Figure 9). Study pH levels were 11, 12, and 13. The NaY zeolite synthesized at pH 13 had the highest H-OH intensity at 1600 cm−1. The results matched energy-dispersive X-ray spectroscopy. Hydroxyl groups have connected to the zeolite structure, as seen by its band at 3460 cm−1. Aluminum oxide compound development is shown by a peak at 1500 cm−1. This shows the aluminasilicate structure collapses, resulting in smaller fragments. The 1636 cm−1 band, typically a deformation band, indicates water absorption in zeolite. Asymmetrical stretch

vibrations in the zeolite's inner tetrahedral structure may cause the peak about 1000 cm−1, while symmetrical stretch vibrations cause peaks between 720 and 650 cm−1.

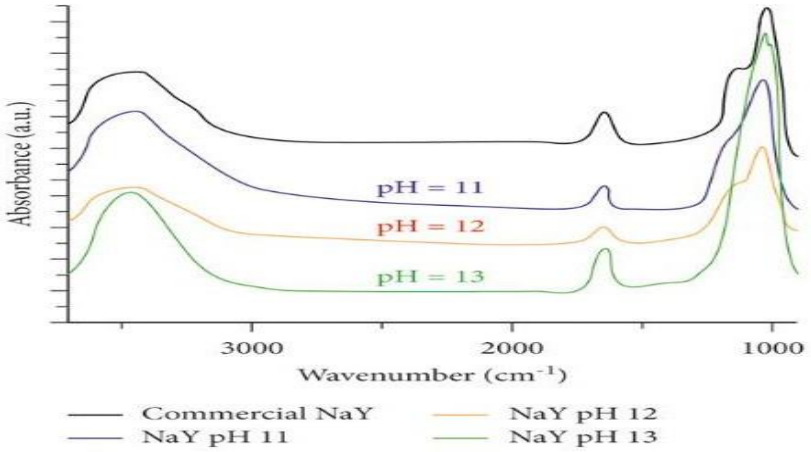

Figure 9 FT-IR spectrum of synthesized zeoliteNaY.

Gaidoumi et al. tested natural and modified clays [24]. Pyrophyllite is seen in the FTIR spectrum. The OH bond stretching and vibration in Al-OH is indicated by absorption peaks at 3674, 854, and 835 cm−1. The peak at 3446 cm−1 may be caused by the O-H bonds of adsorbed water or the stretching of the surface water molecule. The band at 1428 cm−1 indicates carbonate impurities, while the peak at 980 cm−1 is caused by Si-OH's high nonbridging stretching vibration. Quartz is identified by its 797, 779, and 693 cm−1 bands. Si-O-Si bonds vibrate at 518 cm−1, while Si-O groups bend at 440 cm−1. PZ spectra show hydroxyl sodalite vibrational bands. In synthetic HS, peaks between 3000 and 4000 cm−1 are attributed to OH ions in structural water molecules. The signal at 3626 cm−1 in the XRD examination confirms the presence of the hydroxy sodalite (HS) phase with four water molecules. The bands below 1200 cm−1 are caused by the symmetric and antisymmetric vibrations of T-O-T (T=Al and Si). T-O-T asymmetric stretching vibration is indicated by the broad band at 983 cm−1, while symmetric stretching is represented by broad bands at 731 and 663 cm−1. Figure 10 displays the bending vibration of O-T-O as absorption bands at 461 and 433 cm−1.

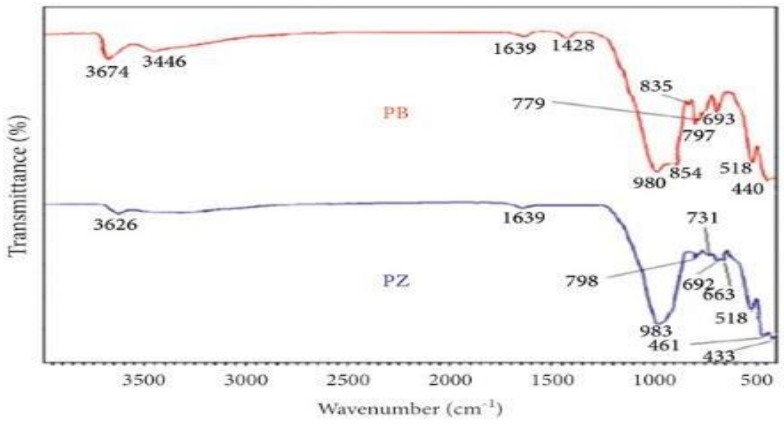

Figure 10 FTIR spectra of samples: natural clay (PB) and pyrophyllite (PZ).

In Figure 11, the FT-IR spectra of natural zeolite indicate the symmetric and asymmetric stretching vibrations of the hydroxyl functional group and Si-O bond at 3614 cm−1 and 1645 cm−1, respectively. Al-O bond vibrations are confirmed by the 1087 cm−1 band. The scientists believe the zeolite has a huge surface area because to its allotropic SiO2 phase at 797 cm−1 and strong tectosilicate linkages between Si, O, and Al.

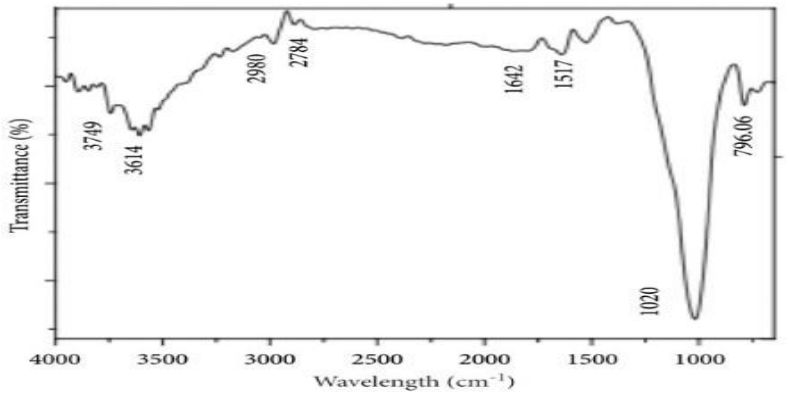

Figure 11 FT-IR spectra of the natural zeolite clinoptilolite type.

CATALYTIC PROPERTIES OF ZEOLITES

Zeolites' catalytic activity comes from bronzed acids on the OH bridging structure between silicon and aluminum channels. Trivalent elements replace Si atoms in zeolite structures, creating a negatively charged lattice charge that needs a positively charged counterion. Brønsted acid sites form with proton charge balance. Bridging hydroxyls develop near Si-O- Al clustering. Scheme 1 shows protons, the negative charge-neutralizing cation. Si-OH-Al sites or hydroxyl groups donate protons.

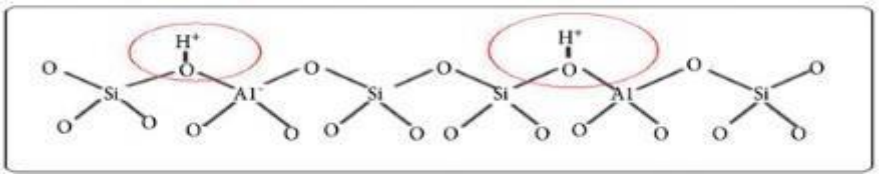

Scheme 1 Brønsted acid sites in zeolites framework.

Esterification using heterogeneous catalyst zeolite A produced ethyl acetate from acetic acid and ethanol. Zeolite moved the equilibrium reaction toward the product by acting as a surfactant and eliminating unwanted molecules (Scheme 2). The adsorbed acetic acid on the zeolite catalyst bonds with ethanol to form water and ethyl acetate by intramolecular dehydration (Scheme 2). Improving the accessibility of bulky molecules to the active sites in zeolite channels and reducing diffusional limitations while maintaining high selectivity and catalytic activity are crucial, but the authors failed to address the causes of poor catalyst utilization and decreased catalytic rate, such as small pore sizes and long diffusion path lengths, which reduce transport efficiency.

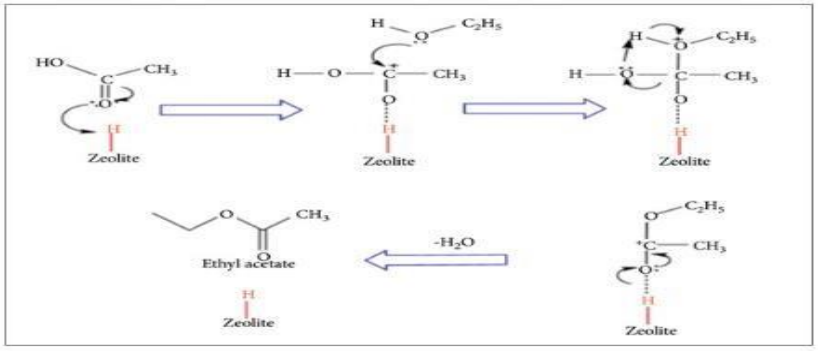

Scheme 2 Vapor-phase acetic acid esterification with ethanol.

In Scheme 3, zeolites are used as a catalyst in transesterification and esterification processes for biodiesel production (Fattahi, 25).

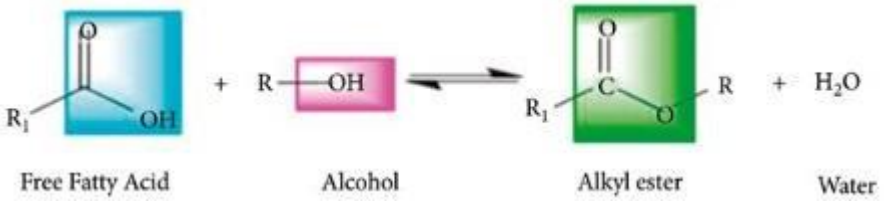

Scheme 3 (a) Production of biodiesel (alkyl ester) via (a) esterification and (b) transesterification reaction.

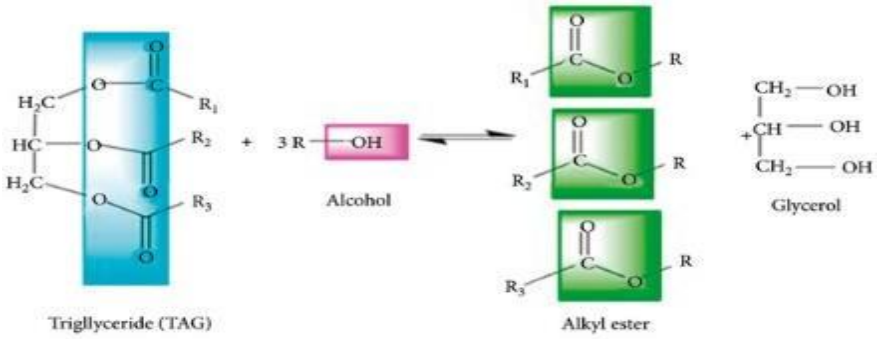

Scheme 3 (b) Production of biodiesel (alkyl ester) via (a) esterification and (b) transesterification reaction.

In Scheme 4, Li et al. [26] used zeolites as catalysts to convert microbe-generated lactic acid into lactide, a renewable and biodegradable polymer. Due to undesirable byproducts from high- temperature condensation and transesterification, typical lactide production from lactic acid takes a lot of energy and time. The authors also ignored impurity aggregation and sintering into the zeolite active site, which reduces catalytic efficacy for reaction coordination.

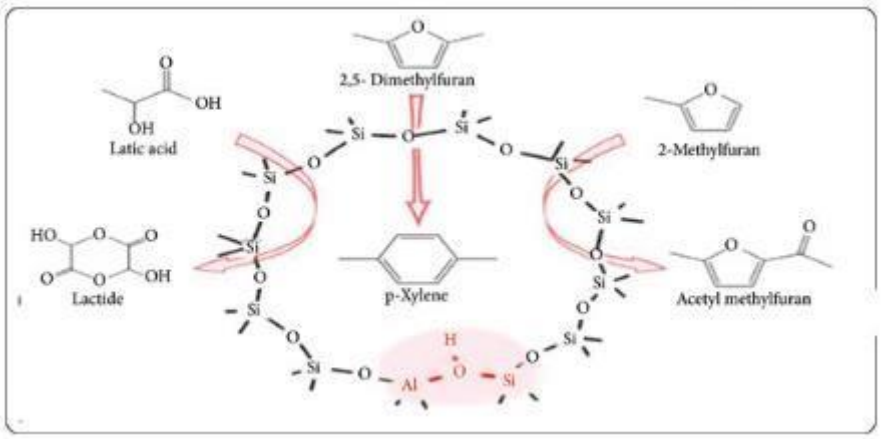

Scheme 4 Reactions over a Brønsted acid site.

Corma et al. [27] state that reaction factors such temperature, reactants, pressure, support, metal loading, and particle size affect catalyst activation and deactivation. Figure 12 shows how metal atoms can migrate between porous zeolite sites via the porous carrier material's channel, pore, or cavity, according to the scientists. (A) The atomicity of metal species can change from individual atoms to clusters of a few atoms or nanoparticles with tens or hundreds of atoms depending on reaction conditions and catalyst physicochemistry. The structural alteration or segregation of supported single-atom alloy nanoparticles may occur due to air changes or reaction conditions. In contrast, chemically segregated bimetallic nanoparticles can be transformed into single-atom alloy nanoparticles under certain reaction conditions.

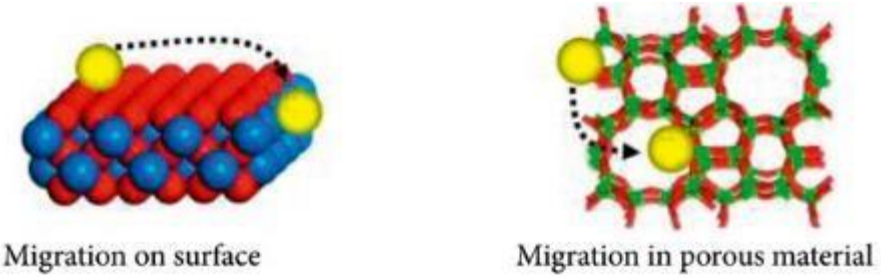

Figure 12 (a) The structures of heterogeneous metal catalysts (a) Change of coordination environment.

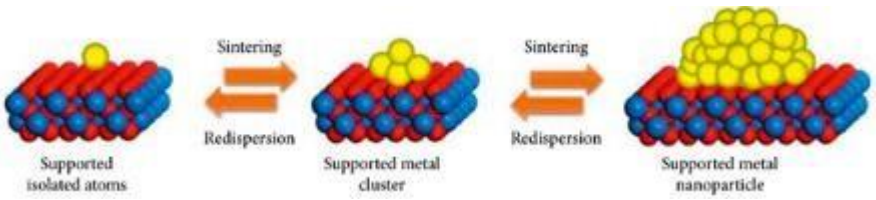

Figure 12 (b) The structures of heterogeneous metal catalysts (b) Change of size.

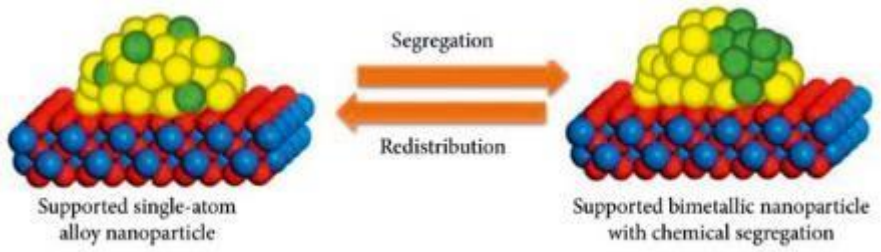

Figure 12 (c) The structures of heterogeneous metal catalysts (c) Change of spatial distribution of the chemical compositions.

Encapsulating transition metals and their complexes in zeolites may boost catalytic activity in many chemical processes. Pan et al. [28] evaluated hierarchical and microporous zeolites to improve catalytic activity and catalyst lifespan for commercial use. Risheng et al. [29] investigated hierarchical zeolites with microporous and mesoporous zeolites to avoid mass- transfer issues with microporous zeolites. Reducing the pore-blocking effect of accumulated coke species and the diffusion and steric limits of bulky molecules improves zeolite catalyst usage efficiency, lifetime, and performance. These synthetic approaches tune hierarchical zeolite features like distribution, dimensionality, connectedness, and secondary pore ordering to increase big molecule mobility and substrate accessibility to catalyst active sites. Hierarchical zeolites can also reduce steric limitations on big molecule conversion, speed up intracrystalline diffusion, avoid coking-induced deactivation, maximize catalyst use, and regulate.

CONCLUSION

In conclusion, the synthesis methods of zeolites are impacted by a number of characteristics, such as the composition of the precursors, the pH of the reaction, the temperature, the pretreatment of the precursors, the seeding time, the reaction time, and the templates that are used. In order to sidestep competitive reactions in a variety of well-established processes, microwave synthesis modalities are currently being utilized widely in specific zeolite synthesises. This is due to the fact that these modalities are both quick and efficient in terms of energy consumption. The sol-gel synthesis approach has further improved the technology for zeolite synthesis by making it easier to effectively encapsulate components (such as metals or metal oxides) into cavities. This has resulted in the technique being further improved. In spite of the fact that a two-step crystallization technique shows promise for the synthesis of hierarchical porous zeolite, another way of synthesis that generates particles that are smaller and more uniform in a shorter amount of time is the combination of hydrothermal crystallization and microwave heating technology. Because of the high product yield and the rapid crystallization rate, it is required to integrate several synthesis processes. Some examples of these approaches are solid-state or quasi-solid-state synthesis that makes use of microwave technology. Nevertheless, the utilization of a hierarchical approach is essential in order to enhance the diffusion and catalytic properties of zeolite materials. This is done in order to prevent the appearance of aggregation and diffusion constraints. To add insult to injury, the application of computational approaches such as density functional theory (DFT), Gaussian, and AOMix provides significant contributions to the clarification of the molecular features of active sites in zeolite catalysts.

REFERENCES

1. Wang S., Peng Y. Natural zeolites as effective adsorbents in water and wastewater treatment. Chem. Eng. J. 2010;156:11–24. doi: 10.1016/j.cej.2009.10.029.
2. Kuldeyev E., Seitzhanova M., Tanirbergenova S., Tazhu K., Doszhanov E., Mansurov Z., Azat S., Nurlybaev R., Berndtsson R. Modifying natural zeolites to improve heavy metal adsorption. Water. 2023;15:2215. doi: 10.3390/w15122215.
3. Lima R.C., Bieseki L., Melguizo P.V., Pergher S.B.C. Environmentally Friendly Zeolites—Synthesis and Source Materials. Springer; Berlin/Heidelberg, Germany: 2019.
4. Walkowiak A., Wolska J., Wojtaszek-Gurdak A., Sobczak I., Wolski L., Ziolek M. Modification of gold zeolitic supports for catalytic oxidation of glucose to gluconic acid. Materials. 2021;14:5250. doi: 10.3390/ma14185250.
5. Szostak R. Molecular Sieves. Principles of Synthesis and Identifiifaction. Springer; New York, NY, USA: 1989.
6. Ming D.W., Allen E.R. Use of natural zeolites in agronomy, horticulture and environmental soil remediation. Rev. Mineral. Geochem. 2001;45:619–654. doi: 10.2138/rmg.2001.45.18.
7. Johnson E.B.G., Arshad S.E. Hydrothermally synthesized zeolites based on kaolinite: A review. Appl. Clay Sci. 2014;97–98:215–221. doi: 10.1016/j.clay.2014.06.005.
8. Novembre D., Sabatino B.D., Gimeno D., Garcia-Vallès M., Martínez-Manent S. Synthesis of Na-X zeolites from tripolaceous deposits (Crotone, Italy) and volcanic zeolitised rocks (Vico volcano, Italy) Microporous Mesoporous Mater. 2004;75:1–11. doi: 10.1016/j.micromeso.2004.06.022.
9. Zhang X., Tong D., Zhao J., Li X. Synthesis of NaX zeolite at room temperature and its characterization. Mater. Lett. 2013;104:80–83. doi: 10.1016/j.matlet.2013.03.131.
10. Aylele L., Pérez-Pariente J., Chebude Y., Díaz I. Conventional versus alkali fusion synthesis of zeolite A from low grade kaolin. Appl. Clay Sci. 2016;132–133:485–490. doi: 10.1016/j.clay.2016.07.019.
11. Lee M.-G., Park J.-W., Kam S.-K., Lee C.-H. Synthesis of Na-A zeolite from Jeju Island Scoria using fusion/hydrothermal method. Chemosphere. 2018;207:203–208. doi: 10.1016/j.chemosphere.2018.05.080.
12. Garcia-Lodeiro J., Maltceva O., Palomo A., Fernandes-Jiménez A. Hybrid alkaline cements: Part I. Fundamentals. Rom. J. Mater. 2012;42:330–335.
13. Villa C., Pecina E.T., Torres R., Gómez L. Geopolymer synthesis using alkaline activation of natural zeolite. Constr. Build. Mater. 2010;24:2084–2090. doi: 10.1016/j.conbuildmat.2010.04.052.
14. Park M., Choi J. Molten-salt method for the synthesis of zeolitic materials I. Zeolite formation in alkaline molten-salt system. Microporous Mesoporous Mater. 2000;37:9. doi: 10.1016/S1387-1811(99)00196-1.
15. Panzarella B., Tompsett G.A., Ynqvesson K.S., Conner W.C. Microwave synthesis of zeolites. 2. Effect of vessel size, precursor volume, and irradiation method. J. Phys. Chem. B. 2007;111:12657–12667. doi: 10.1021/jp072622d.
16. Anuwattana R., Balkus K.J., Jr., Asavapisit S., Khummongkol P. Conventional and microwave

hydrothermal synthesis of zeolite ZSM-5 from the cupola slag. Microporous Mesoporous Mater. 2008;111:260–266. doi: 10.1016/j.micromeso.2007.07.039.

17. Kim M.-H., Li H.-X., Davis M.E. Synthesis of zeolites by water-organic vapor-phase transport. Micropor. Mater. 1993;1:191–200. doi: 10.1016/0927-6513(93)80077-8.
18. Melaningtyas G. S. A., Krisnandi Y. K., and Ekananda R., Synthesis and characterization of NaY zeolite from Bayat natural zeolite: effect of pH on synthesis, Materials Science and Engineering.(2019) **496**, 1–5, **https://doi.org/10.1088/1757-899x/496/1/012042**, 2-s2.0-85066912545.
19. Chunfeng W., Jiansheng L., Xia S., Lianjun W., and Xiuyun S., Evaluation of zeolites synthesized from fly ash as potential adsorbents for wastewater containing heavy metals, Journal of Environmental Sciences.(2009) **21**, 127–136, **https://doi.org/10.1016/S1001-0742(09)60022-X**, 2-s2.0-58149523098.
20. Magdalena L., Synthesis, Characterization and Properties of Zeolite Films and Membranes, 2001, Lulea University of technology, Luleå, Sweden.
21. Omisanya N. O., Folayan C. O., Aku S. Y., and Adefila S. S., Synthesis and characterization of zeolite a for adsorption refrigeration application, Advances in Applied Science Research. (2012) **6**, 3746–3754.
22. Nyankson E., Efavi J.K., Yaya A., Manu G., Asare K., and Daafuor J., Synthesis and characterization of zeolite-A and Zn-exchanged zeolite-A based on natural aluminosilicates and their potential applications, Cogent Engineering. (2018) **5**, 1– 23, **https://doi.org/10.1080/23311916.2018.1440480**, 2-s2.0-85044145164.
23. Wang C., Shi H., and Li Y., Synthesis and characterization of natural zeolite supported Cr-doped TiO2 photocatalysts, Applied Surface Science. (2012) **258**, no. 10, 4328–4333, **https://doi.org/10.1016/j.apsusc.2011.12.108**, 2-s2.0-84862801883.
24. Gaidoumi A. El, Benabdallah A. C., Bali B. E., and Kherbeche A., Synthesis and characterization of zeolite HS using natural pyrophyllite as new clay source, Arabian Journal for Science and Engineering. (2011) **43**, 1–8, **https://doi.org/10.1007/s13369-017-2768-8**, 2-s2.0-85039919441.
25. Fattahi N., Zeolite-based catalysts: a valuable Approach toward ester bond formation, 2019, **9**, 1–23, **https://doi.org/10.3390/catal9090758**, 2-s2.0-85073334097.
26. Li Y., Li L., and Yu J., Applications of zeolites in sustainable chemistry, Inside Cosmetics. (2017) **3**, no. 6, 928–949, **https://doi.org/10.1016/j.chempr.2017.10.009**, 2-s2.0-85038237435.
27. Corma L., Lichen L., and Avelino C., Evolution of isolated atoms and clusters in catalysis, Trends in Chemistry.(2020) **2**, 383–400, **https://doi.org/10.1016/j.trechm.2020.02.003**.
28. Pan T., Wu Z., Alex C., and Yip K., Advances in the green synthesis of microporous and hierarchical zeolites: a short review, Catalysts.(2019) **9**, 1– 18, **https://doi.org/10.3390/catal9030274**, 2-s2.0-85064197461.
29. Risheng B., Yue S., Yi L., and Jihong Y., Creating Hierarchical pores in zeolites catalyst, Trends in Chemistry.(2019) **1**, 601–611, **https://doi.org/10.1016/j.trechm.2019.05.010**, 2-s2.0-85069733909.